A New Cobaltite with a Tubular Structure: $Bi_{3.7}Sr_{11.4}Co_8O_{28-\delta}$, the $n = 2$ Member of the Series $[Bi_2Sr_2CoO_6]_n[Sr_8Co_6O_{16-\delta}]$

D. Pelloquin,* A. C. Masset, A. Maignan, C. Michel, M. Hervieu, and B. Raveau

Laboratoire CRISMAT, CNRS UMR 6508, ISMRA, 6 Boulevard du Maréchal Juin, 14050 Caen Cedex, France

Received June 30, 1998. Revised Manuscript Received September 30, 1998

A cobaltite, $Bi_{3.7}Sr_{11.4}Co_8O_{28-\delta}$, with a "tubular" structure derived from the 2201-type has been synthesized for the first time. This oxide represents, like the homologous manganese phase, the $n = 2$ member of the large structural $[Bi_2Sr_2MO_6]_n[Sr_8M_6O_{16\pm\delta}]$ family (M = Cu, Co, Mn). Although its structure is similar to the Mn phase, it crystallizes in a different space group, *Ammm* (or *Amm*2), with $a = 5.5232(2)$ Å, $b = 23.465(1)$ Å, and $c = 23.462(1)$ Å. The HREM study confirms that the structure consists of the stacking along *b* (or *c*) of "2201"-type slices with single cobalt-deficient perovskite slices $[Sr_8Co_6O_{16-\delta}]$. But the important difference with the Mn phase concerns the nature of the "Co_4" pillars, which are at the intersection of two $[Sr_8Co_6O_{16-\delta}]$ slices. They form four corner-sharing CoO_4 tetrahedra instead of MnO_6 octahedra and MnO_5 pyramids. This structural difference means that the Mn and Co phases do not form a complete solid solution. The tubular series $Bi_{4-y}Sr_{12-z}Mn_{8-x}Co_xO_{28\pm\delta}$ could only be obtained for $0 \le x \le 2.5$. The magnetic properties of this oxide are very complex and are very sensitive to the oxygen content. In particular, after oxygen pressure annealing, they are characteristic of spin-state transitions with temperatures close to 50 and 450 K, similar to those observed in the $LaCoO_3$ compound.

Introduction

After the discovery of the first tubular structure $Bi_4Sr_8Cu_5O_{19+\delta}$, by Fuertes et al.,[1] the investigation of the Bi−Sr−Cu−O system allowed a large structural series to be evidenced, with the formula $[Bi_2Sr_2CuO_6]_n[Sr_8Cu_6O_{16+\delta}]$.[2] The different members of this series, $n = 4$, 5, 6, 7, derive from the structure of the 2201 superconductor $Bi_2Sr_2CuO_{6+\delta}$.[3,4] They are built up of 2201-type slices which are *n* octahedra wide along *b* and interconnected through single perovskite related layers, "$Sr_8Cu_6O_{16+\delta}$". In fact, these structures can be described as monolayers of criss-crossing CuO_6 octahedra forming tubes where the [BiO] rows are interpolated. At the intersection of the octahedral monolayers, the copper polyhedra are oxygen deficient so that oxygen deficient pillars built up of four Cu polyhedra (the "Cu_4" pillars) are formed.

Taking into consideration the fact that such original frameworks may be stabilized thanks to the Jahn−Teller effect of copper, the Bi−Sr−Mn−O system was recently investigated and a new manganite, $Bi_{3.6}Sr_{12.4}Mn_8O_{28.9}$, with a tubular structure was isolated.[5] This phase, which corresponds to the $n = 2$ member of the $[Bi_2Sr_2MnO_{6+\delta}]_n[Sr_8Mn_6O_{16+\delta}]$ generic family, has never been stabilized by copper. The reasons could be due to the necessity for the transition metal to increase dramaticaly its mean oxidation state, when *n* decreases, to limit the presence of oxygen defiency in the metal−oxygen framework and to the difficulty to stabilize trivalent copper. In contrast, other members of the series ($n > 3$) were not synthesized to date in the Bi−Sr−Mn−O system. At this point of the investigations, the factors which govern the stabilization of such frameworks are not understood, and the possibility to form such oxides with cations other than copper and manganese has to be considered, also bearing in mind the possibility to generate new magnetic properties. For this reason, we have investigated the Bi−Sr−Co−O system. We report herein on the first cobaltite that exhibits a tubular structure. We show that this phase, with the formula $Bi_{4-y}Sr_{12-z}Co_8O_{28-\delta}$, corresponds to the $n = 2$ member of a large tubular family, like the corresponding manganite $Bi_{3.6}Sr_{12.4}Mn_8O_{28.9}$, but differs from the latter by the nature of the CoO_n polyhedra forming the "Co_4" pillars. The possibility of building up a solid solution between the Mn and Co phases was also investigated. The study of the magnetic properties of these oxides shows an antiferromagnetic behavior at low temperature and emphasizes the possible appearance of an intermediate spin-state transition in the pure

(1) Fuertes, A.; Miravitlles, C.; Gonzalez-Calbet, J.; Vallet-Regi, M.; Obradors, X.; Rodriguez-Carvajal, J. *Physica C* **1989**, *157*, 525. Caldes, M. T.; Navarro, J. M.; Perez, F.; Carrera, M.; Fontcuberta, J.; Casan-Pastor, N.; Miravitlles, C.; Obradors, X.; Rodriguez-Carvajal, J.; Gonzalez-Calbet, J.; Vallet-Regi, M.; Fuertes, A. *Chem. Mater.* **1991**, *3*, 844.

(2) Caldes, M. T.; Hervieu, M.; Fuertes, A.; Raveau, B. *J. Solid State Chem.* **1992**, *97*, 48.

(3) Michel, C.; Hervieu, M.; Borel, M. M.; Grandin, A.; Deslandes, F.; Provost, J.; Raveau, B. *Z. Phys. B* **1987**, *68*, 421.

(4) Torrance, J. B.; Tokura, Y.; La Placa, S. J.; Huang, T. C.; Savoy, R. J.; Nazzal, A. I. *Solid State Commun.* **1988**, *66*, 703.

(5) Pelloquin, D.; Michel, C.; Maignan, A.; Hervieu, M.; Raveau, B. *J. Solid State Chem.* **1998**, *138*, 278.

10.1021/cm980467x CCC: $18.00
Published on Web 12/15/1998

cobalt-based tubular phase according to the global oxygen content.

Experimental Section

The system Bi−Sr−Co−O was first investigated, using the generic formula $[Bi_2Sr_2CoO_6]_n[Sr_8Co_6O_{16+\delta}]$ for the starting compositions. In a similar way, attempts to replace partly Mn by Co in the $n = 2$ member were made from the ideal composition $Bi_4Sr_{12}Mn_{8-x}Co_xO_{28+\delta}$ by varying x from 0 to 8. All the samples were prepared by solid-state reaction between Bi_2O_3, SrO_2/SrO, Mn_2O_3/Mn, and Co_3O_4/Co precursors weighted in the stoichiometric proportions. To avoid the carbonate contamination, SrO oxide was freshly prepared by heating SrO_2 peroxide or $Sr(OH)_2{\cdot}8H_2O$ hydrated hydroxide at 1000 °C. The mixtures, intimately ground in an agate mortar, were placed in an alumina finger. This step was performed in a drybox. Next, the mixtures were sealed in an evacuated silica ampule and heated to a temperature close to 950 °C, at 150 °C h^{-1}, kept at this temperature for 24 h, and cooled to room temperature, at 150 °C h^{-1}.

The electron diffraction (ED) studies were carried out, using a JEOL 200 CX microscope fitted with an eucentric goniometer (±60°), whereas the high-resolution electron microscopy (HREM) images were performed with a topcon 002B microscope operating at 200 kV and having a point resolution of 1.8 Å. HREM image calculations were carried out with the Mac-Tempas multislice program. Both microscopes are equipped with an EDX analyzer.

X-ray patterns were collected using a Philips vertical diffractometer, equipped with a secondary graphite monochromator and working with the Cu Kα radiation. Data collection was performed by step scanning over an angular range $5° \leq 2\theta \leq 100°$ and next the data were treated by profile analysis with the program Fullprof (version 3.2).[6]

Magnetic susceptibility $\chi(T)$ measurements were investigated at low temperature (5−300 K) using a AC-DC SQUID Quantum Design magnetometer (ZFC method) and at high temperature (300−800 K) using the Faraday method with, in the both cases, an applied field of 3 kG. Resistivity measurements were recorded with a physical properties measurements system (PPMS) from Quantum Design (four-probe method).

Results and Discussions

I. The Cobaltite $Bi_{3.7}Sr_{11.4}Co_8O_{26.8}$. Under the above experimental conditions, the study of the system Bi−Sr−Co−O allowed stabilization of a new phase whose X-ray powder diffraction pattern (Figure 1) shows close structural relationships with that of the tubular phase $Bi_{3.6}Sr_{12.4}Mn_8O_{28.9}$.[5] The EDX analyses performed on numerous microcrystals led to an average cationic composition close to "$Bi_{3.7}Sr_{11.4}Co_8$", supporting that this structure is similar to that previously reported for the manganite $Bi_{3.6}Sr_{12.4}Mn_8O_{28.9}$.[5] On this basis and assuming Bi^{3+}, the oxygen content, determined by usual redox titration, was found to be 26.8(1), leading to a formal oxidation state close to +2.5 for cobalt. The ED patterns of this new cobaltite (Figure 2c,d) show a set of intense reflections, leading to a pseudotetragonal cell with the parameters $a \approx a_p\sqrt{2} \approx 5.5$ Å, $b \approx 23.5$ Å, and $c \approx 23.5$ Å, similar to that observed for $Bi_{3.6}Sr_{12.4}Mn_8O_{28.9}$ (Figure 2a,b); the conditions limiting the reflections are compatible with the orthorhombic space groups *Fmmm* and *Fmm*2. However, both oxides exhibit a set of weak extra reflections (see white arrows Figure 2a,b for Mn and Figure 2c,d for Co). As can be seen in the

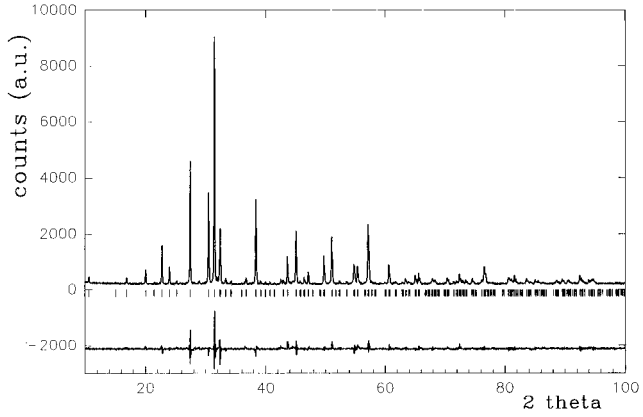

Figure 1. Experimental and difference powder X-ray diffraction patterns of the tubular phase $Bi_{3.7}Sr_{11.4}Co_8O_{26.8}$. Vertical bars indicate the Bragg angle positions calculated from *Fmmm* space group with $a = 5.5232(2)$ Å, $b = 23.465(1)$ Å, and $c = 23.462(1)$ Å.

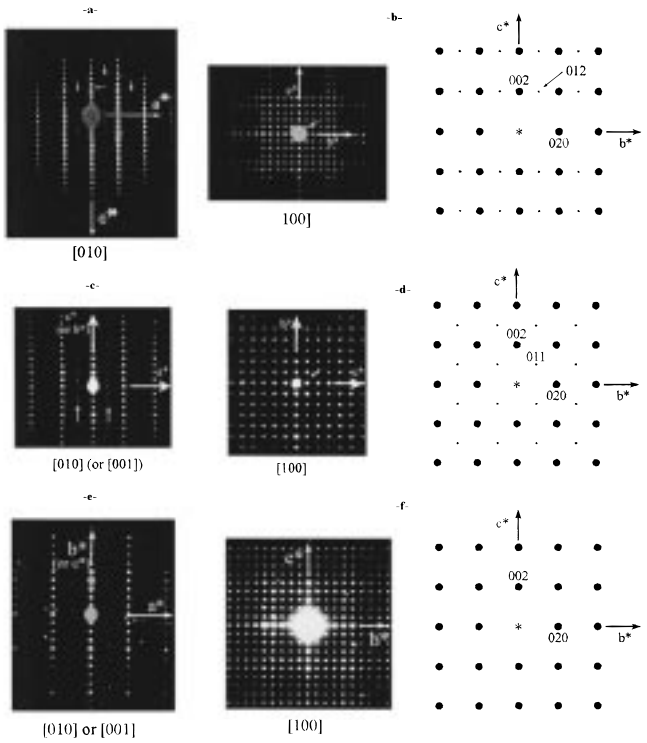

Figure 2. Experimental and schematic ED patterns oriented [010] and [100] corresponding to (a, b) $Bi_{3.6}Sr_{12.4}Mn_8O_{28.9}$, (c, d) $Bi_{3.7}Sr_{11.4}Co_8O_{26.8}$, (e, f) $Bi_{3.95}Sr_{11.7}Mn_{5.6}Co_{2.4}O_{28\pm\delta}$.

[100] (Figure 2b,d) and [010] ED patterns (Figure 2a,c), the systems of extra reflections are different in the Mn and Co phases. Considering the extra reflections, the reconstruction of the reciprocal space for the cobaltite leads to an actual orthorhombic crystallographic cell with the possible space groups *Ammm* and *Amm*2, whereas the space group *Pbnb* was observed for the Mn phase.[5]

A comparative HREM study has been carried out in order to explain this difference between Mn and Co phases. Typical [100] HREM images of the two phases have been recorded and are compared in Figure 3. In both, the zones of high electron density are imaged as bright dots, and a regular contrast is observed, consisting in a regular paving of square blocks of 4 × 4 bright dots. It has been previously shown that they are

(6) Rodriguez-Carvajal, J. In *Collected Abstract of Powder Diffraction Meeting*; Galy, J., Ed.; 1990; p 127.

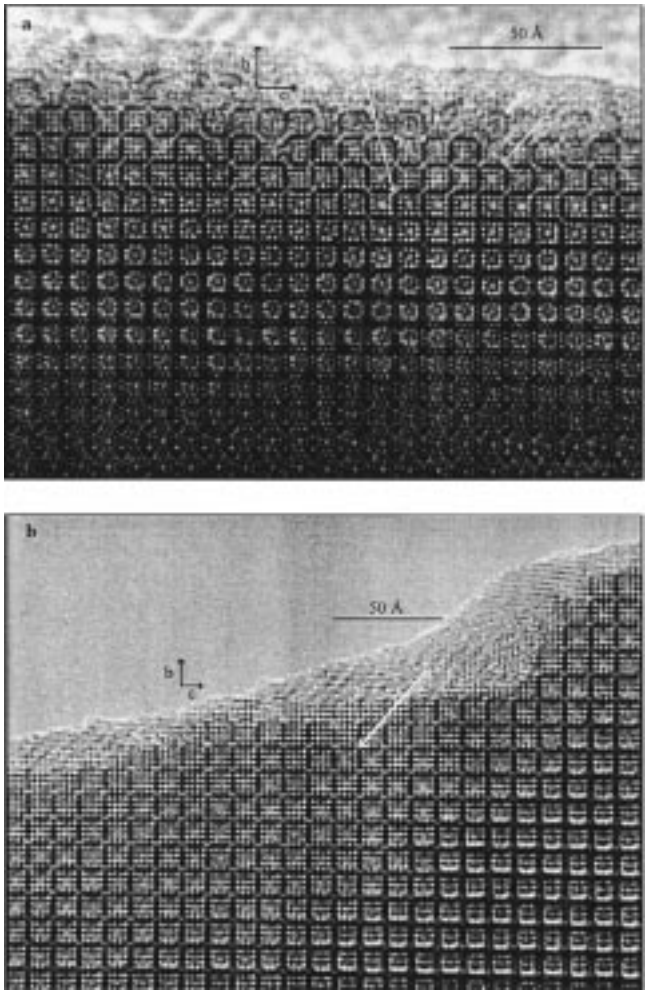

Figure 3. Experimental HREM images recorded along [100] direction for $Bi_{3.6}Sr_{12.4}Mn_8O_{28.9}$ and $Bi_{3.7}Sr_{11.4}Co_8O_{26.8}$. Bright dots are correlated to Bi and Sr atoms and pillars are indicated with white arrows.

correlated to the positions of Bi and Sr atoms in the Mn tubular phase.[5] The observations confirm that the cobaltite phase exhibits a cationic framework similar to that of the manganite. Each block of 4 × 4 bright dots is separated along *b* and *c* by dark rows associated with $[MnO_2]_\infty$ or $[CoO_2]_\infty$ layers. Thus, this contrast is in agreement with the structural model shown in Figure 4, where the criss-crossing layers of MnO_6 or CoO_6 octahedra form tubes in which the [BiO] rows are running. The remarkable character of this structure is that it exhibits 90° oriented "2201"-type slices, in agreement with its pseudotetragonal symmetry, for cobalt as well as for manganese. The main difference of contrast between the cobalt- and manganese-based tubulars stays at the level of pillars that are formed at the intersection of the octahedral layers, as clearly observed in the thin edges of the crystallites (see white arrows in Figures 3). For the cobalt-based phase (Figure 3b), the contrast is symmetric with a 4-fold-type symmetry forming cross shaped gray dots, while in the case of the $Bi_{3.6}Sr_{12.4}Mn_8O_{28.9}$ phase (Figure 3a), the contrast is asymmetric and consists of one elongated gray dot along one of the pillar diagonals. This suggests that the structural difference between the Co and Mn phases is closely related to the nature of the MO_n polyhedra forming these pillars and, in particular, to the content and position of the oxygens inside the latter.

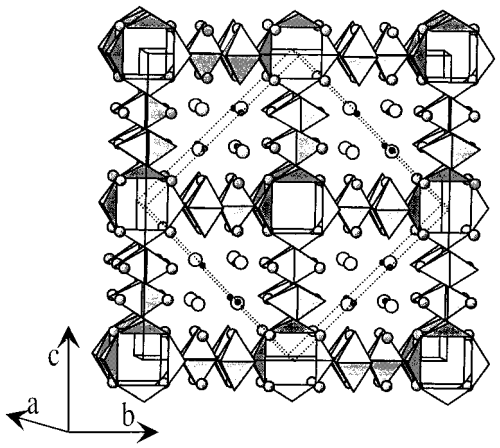

Figure 4. General view of the structure of the tubular-2 phase. The unit cell $a_p\sqrt{2} \times 23.5 \times 23.5$ Å^3 is outlined with solid lines, whereas dotted lines show the possible tetragonal unit cell $16.6 \times 16.6 \times a_p\sqrt{2}$ Å^3.

Table 1. Refined Variable Parameters

atom	site	*x*	*y*	*z*	B(Å^2)	*n*
Bi	16m	0	0.3100(4)	0.1923(3)	0.3(1)	15.2(2)
Co(1)	8h	0	0.086(2)	0	1.2(2)	8
Co(2)	8h	0	0.307(2)	0	1.2(2)	8
Co(3)	8i	0	0	0.084(1)	1.2(2)	8
Co(4)	8i	0	0	0.305(1)	1.2(2)	8
Sr(1)	16m	0	0.1965(8)	0.0760(5)	0.16(8)	13.6(2)
Sr(2)	16m	0	0.0794(6)	0.4151(5)	0.16(8)	16
Sr(3)	16m	0	0.0814(6)	0.1957(5)	0.16(8)	16
O(1)	32p	0.091(2)	0.191(4)	0.180(5)	0.9(3)	16
O(2)	16o	0.275(8)	0.130(3)	0	0.9(3)	16
O(3)	8e	0.25	0.25	0	0.9(3)	8
O(4)	16n	0.277(8)	0	0.139(2)	0.9(3)	16
O(5)	8d	0.25	0	0.25	0.9(3)	8
O(6)	16m	0	0.291(3)	0.101(2)	0.9(3)	16
O(7)	16m	0	0.091(3)	0.086(2)	0.9(3)	16
O(8)	16m	0	0.083(3)	0.307(2)	0.9(3)	16
O(9)	4b	0.5	0	0	0.9(3)	3.5(5)

space group	cell parameters	*R* factors
Fmmm (No. 69)	$a = 5.5232(2)$ Å	$R_p = 0.128$
	$b = 23.465(1)$ Å	$R_{wp} = 0.166$
	$c = 23.462(1)$ Å	$R_I = 0.085$

The estimated standard deviations refer to the last digit.

To check the above hypothesis, a structural study was performed from powder X-ray diffraction data. In the *Ammm* space group, more than 30 independent atoms are necessary to describe the structure, which involve more than 40 variable parameters. We thought that the last number was too high with regard to the information we could obtain from powder X-ray diffraction data. For this reason we preferred to use a more symmetrical space group, i.e., *Fmmm*. Note that this space group was also used for the average structure of the $Bi_{3.6}Sr_{12.4}Mn_8O_{28.9}$ manganese-based tubular.[5] The starting positional parameters were deduced from results obtained for the latter structure. First, the pillars were assumed free of occupancy. Some variable positional parameters for oxygen atoms were fixed in order to decrease the number of independent variable parameters (see Table 1). For the same reason an overall isotropic temperature factor was considered for each kind of ion. To take in account the cationic content issued from EDX analysis, occupancy factors of crystal-

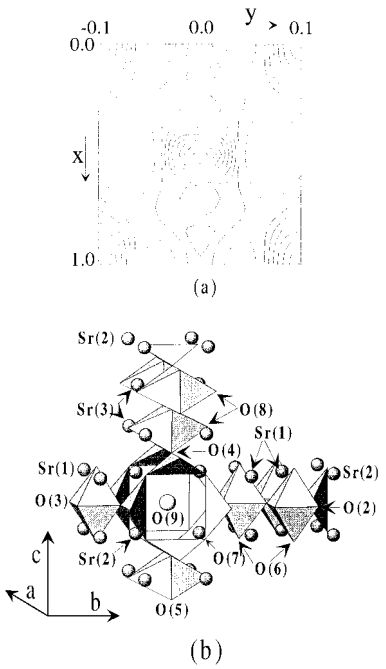

Figure 5. (a) Fourier difference map section at $z = 0$ showing an electronic residue at $x = 0.5$ and $y = 0$. (b) Schematic view of a part of the cobalt−oxygen framework. Strontium atoms (grey circles) and oxygen O(9) are also drawn.

lographic sites were refined for bismuth and strontium. When the deviation from the theoritical value was too low to be significant, the occupancy was fixed to the theoritical value and then not refined (Sr(2)−Sr(3)). At this stage, a Fourier difference analysis evidences clearly a peak in ($^1/_2$ 0 0; 4b site) (Figure 5a). This residual electronic density could be attributed to the oxygen inside the pillars (labeled O(9)), despite the oxygen content being lower than 28 per cell. This implies the presence of vacancies on the oxygen crystallograpic sites, as observed in the case of Cu tubular 4[1] and Mn tubular 2.[5] On this basis, the refinement of the O(9) site occupancy leads to 3.5(6) oxygen atoms. The position of this oxygen atom in the pillars differs from the one observed in the ($^1/_4$ 0.03 0.01) position in the case of the Mn-based tubular,[5] in agreement with the contrasts observed by HREM. The final refined variable parameters are listed in Table 1, corresponding to an agreement factor calculated on the intensities, $R_I = 0.085$, and to the difference X-ray powder diffraction pattern shown in Figure 1. Note that the refined cationic composition remains close to that obtained from EDX analysis. These results do not allow determination of the oxygen positions with accuracy and the oxygen content, but they confirm that the average structure of this oxide is similar to that of the manganite. Assuming no oxygen vacancies in the CoO_n framework, the calculated interatomic distances (Table 2) evidence highly distorted octahedral environment for cobalt atoms which do not participate to the pillars (Co(2) and Co(4)) as observed in the manganite. For the cobalt atoms forming the pillar (Co(1) and Co(3)) the situation is different; they can be described as four corner-sharing distorted tetrahedra, as shown in Figure 5b. The difference with the manganite results from the displacement of the oxygen inside the pillars. In the Mn phase, the oxygen atoms belong to the manganese polyhedra; they lie at $x = \pm^1/_4$ and are slightly displaced along [011] and [0$\bar{1}$1] alternately, whereas in the Co phase they are located in $^1/_2$ 0 0. The displacement along $\vec{a}$ is responsible for the tetrahedral coordination of Co(1) and Co(3) and for the increase of the number of oxygen atoms surrounding Sr(2). However the exact nature of the pillar should be determined by neutron or single-crystal X-ray diffraction study.

Table 2. Selected Interatomic Metal−Oxygen Distances (in angstroms)

Bi−O Distances					
Bi−O(1)	×1	2.27(1)			
Bi−O(1)	×1	2.85(5)			
Bi−O(6)	×1	2.18(4)			
Bi−O(8)	×1	2.51(1)			
Sr−O Distances					
Sr(1)−O(1)	×1	2.51(5)	Sr(2)−O(7)	×2	2.77(1)
Sr(1)−O(2)	×2	2.81(5)	Sr(2)−O(8)	×1	2.54(1)
Sr(1)−O(3)	×2	2.58(1)	Sr(2)−O(9)	×1	2.73(1)
Sr(1)−O(6)	×1	2.30(6)	Sr(3)−O(1)	×1	2.64(5)
Sr(1)−O(6)	×2	2.84(1)	Sr(3)−O(4)	×2	2.78(3)
Sr(1)−O(7)	×1	2.49(6)	Sr(3)−O(5)	×2	2.68(1)
Sr(2)−O(2)	×2	2.63(4)	Sr(3)−O(7)	×1	2.57(4)
Sr(2)−O(4)	×2	2.54(3)	Sr(3)−O(8)	×1	2.61(1)
Sr(2)−O(6)	×1	3.07(7)	Sr(3)−O(8)	×2	2.76(1)
Co−O Distances					
Co(1)−O(2)	×2	1.83(5)	Co(3)−O(4)	×2	2.00(5)
Co(1)−O(7)	×2	2.03(4)	Co(3)−O(7)	×2	2.13(6)
Co(2)−O(2)	×2	1.93(7)	Co(4)−O(4)	×2	1.79(5)
Co(2)−O(3)	×2	1.92(4)	Co(4)−O(5)	×2	1.90(2)
Co(2)−O(6)	×2	2.40(4)	Co(4)−O(8)	×2	1.94(1)

II. The Solid Solution $Bi_4Sr_{12}Mn_{8-x}Co_xO_{28\pm\delta}$. To understand the different structural features between the manganese- and cobalt-based tubulars, the system $Bi_4Sr_{12}Mn_{8-x}Co_xO_{28\pm\delta}$ was scanned. Preliminary X-ray studies performed to check the purity of the resulting samples show that single-phased samples are only obtained over a small x homogeneity range and for nominal oxygen stoichiometry in the range from O_{28} to O_{30}. To clarify theses substitutions, in particular the actual cationic compositions and the evolution of cell parameters, all these materials have been studied simultaneously by X-ray and electron diffraction (ED) data coupled with EDX analyses. This work evidences a limited solid solution $Bi_{4-y}Sr_{12-z}Mn_{8-x}Co_xO_{28\pm\delta}$ with x in the range from 0 to 2.5. The refined cell parameters and the cationic composition of different samples are given in Table 3. The $Bi_{3.7}Sr_{11.4}Co_8O_{26.8}$ phase shows a larger a parameter and lower b and c parameters with regard to $Bi_{3.6}Sr_{12.4}Mn_8O_{28.9}$, resulting in a smaller cell volume. In contrast, Co-doped manganite is characterized by a larger cell volume which reaches its maximum around $x = 2$. This might indicate a structural change and explains the limited solid solution despite the existence of the two closely related limit compounds. The second important feature concerns the limit composition $Bi_{3.95}Sr_{11.7}Mn_{5.6}Co_{2.4}O_{28\pm\delta}$. The analyses of the corresponding ED patterns (Figure 2e,f) evidence reflection conditions compatible with the orthorhombic space group $Fmmm$ (or $Fmm2$), in agreement with those previously reported for the intense reflections of $Bi_{3.6}Sr_{12.4}Mn_8O_{28.9}$[5] and $Bi_{3.7}Sr_{11.4}Co_8O_{26.8}$ [this work], but contrary to the latter, any extra reflections violating the F-type lattice have been detected along the [100] direction. Note that this sample, taking account the refinement of cell parameters, can be also described in an actual tetragonal cell with $a \approx 23.5/\sqrt{2} \approx 16.6$ Å and $c \approx a_p\sqrt{2}$ Å and the space group $I4/mmm$ (see dotted line

Table 3. Analytical Results (EDX), Refined Lattice Parameters, and Cell Volume for $Bi_{4-y}Sr_{12-z}Mn_{8-x}Co_xO_{28\pm\delta}$

M	nominal composition	actual cationic composition (EDX)	*a* (Å)	*b* (Å)	*c* (Å)	*V* (Å^3)
Mn[a]	$Bi_4Sr_{12}Mn_8O_{28+\delta}$	$Bi_{3.6}Sr_{12.4}Mn_8O_{28+\delta}$	5.4956(1)	23.595(1)	23.580(1)	3056.7
Co[b]	$Bi_4Sr_{12}Mn_7CoO_{28+\delta}$	$Bi_{3.7}Sr_{11.4}Mn_{7.3}Co_{0.7}O_{28\pm\delta}$	5.5023(1)	23.590(2)	23.575(2)	3060.4
Co[b]	$Bi_4Sr_{12}Mn_6Co_2O_{28+\delta}$	$Bi_{3.8}Sr_{12}Mn_{6.1}Co_{1.9}O_{28\pm\delta}$	5.5387(1)	23.566(2)	23.566(2)	3076.0
Co[b]	$Bi_4Sr_{12}Mn_4Co_4O_{28+\delta}$	$Bi_{3.9}Sr_{11.7}Mn_{5.6}Co_{2.4}O_{28\pm\delta}$	5.5307(1)	23.556(1)	23.558(2)	3069.2
Co[b]	$Bi_4Sr_{12}Co_8O_{28+\delta}$	$Bi_{3.7}Sr_{11.4}Co_8O_{28-\delta}$	5.5231(1)	23.466(2)	23.464(2)	3041.0

[a] From ref 5. [b] From this work.

in Figure 4). So the possibility of a structural transition deduced from the variation of the lattice constants is confirmed by the ED study performed on $Bi_{4-y}Sr_{12-z}Mn_{8-x}Co_xO_{28\pm\delta}$ phases which exhibit different extra reflections along the [100] direction (small white arrow in Figure 2); therefore different space groups are observed according to the *x* values: a *P*-type orthorhombic lattice ($a \approx a_p\sqrt{2} \approx 5.5$ Å, $b \approx 23.59$ Å, and $c \approx 23.58$ Å) for $0 \leq x < 2$, a pseudotetragonal lattice with reflection conditions compatible with the space group *Fmmm* for $2 \leq x \leq 2.5$ and *Ammm* for the pure cobalt phase ($a \approx a_p\sqrt{2} \approx 5.52$ Å, $b \approx 23.45$ Å, and $c \approx 23.45$ Å). Note that a similar structural behavior has been observed in the parent 2201-type phase $Bi_2Sr_2MO_{6+\delta}$ (M = Mn, Co), which exhibits specific space groups according to M cation, *Pmma* and *I*2*mb* for M = Mn and Co respectively.[7,8] Thus the symmetry can be correlated either to the nature of M cationic site and/or to the global oxygen stoichiometry.

III. Magnetic Properties of $Bi_{3.7}Sr_{11.4}Co_8O_{28-\delta}$. To get some supplementary information on the pure cobaltite tubular, magnetic susceptibility $\chi(T)$ measurements were performed in the range 5−800 K. This new cobaltite exhibits very complex magnetic properties. Moreover, the latter are very sensitive to oxygen pressure annealings. This point is illustrated in Figure 6 by the *T*-dependent susceptibility χ curves of the as-synthesized (Figure 6a) and high-pressure oxygen annealed (Figure 6b, PO_2 = 100 bar, T = 450 °C, 12 h) samples. The $\chi(T)$ curve of the Co tubular as-synthesized is characterized by a transition toward a less magnetic state below 75 K. The Curie−Weiss fitting of the corresponding $\chi^{-1}(T)$ curve in the high-temperature range (400−800 K) (inset of Figure 6a), according to the general formula $\chi = \chi_0 + C/(T - \theta_p)$, where C, θ_p, and χ_0 are the Curie constant, the paramagnetic Curie temperature, and the temperature-independent susceptibility, respectively, leads to a negative $\theta_p = -45$ K value and an effective paramagnetic moment of 3.4 μ_B. This value is close to that observed in the parent $Bi_2Sr_2CoO_{6+\delta}$ structure (μ_{eff} = 3.01 μ_B).[8] Even if caution must be exercised in interpreting this value, a formal valence close to 2.5 for cobalt has been proposed in ref 8 further to the structural discussion. Such a hypothesis could be available for this tubular phase taking into account our chemical analysis by redox titration and our structural study which evidences two kinds of CoO_n polyhedra (50% of octahedra and 50% of tetrahedra). The $\chi(T)$ curve shape and the θ_p value suggest that an antiferromagnetic transition occurs or that the Co spin-state changes toward a lower spin-state. Moreover, the

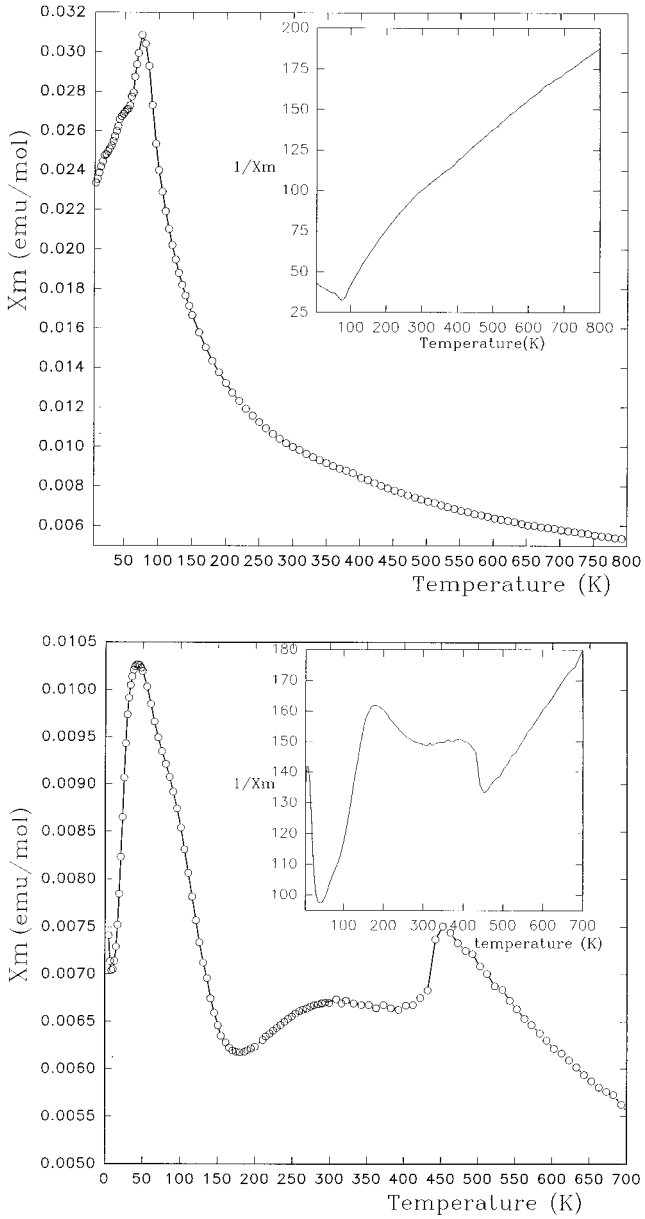

Figure 6. Temperature dependence of the molar magnetic susceptibility χ_M for the as-synthesized (a) and oxygen pressure annealed (b) tubular-2 cobalt phase. Insets show the $\chi_M - 1 = f(T)$ curves.

oxygen pressure annealed sample exhibits a $\chi(T)$ curve showing a great complexity with an additional magnetic transition at about 450 K (Figure 6b). Note that the μ_{eff} = 5.2 μ_B value ($\theta_p = -365$ K), deduced from $\chi^{-1}(T)$ curve fitting (450−800 K), is close to the experimental value observed in the case of a pure high-spin trivalent cobalt (μ_{exp} = 5.4 μ_B).[12] This μ_{eff} increase between the

(7) Tarascon, J. M.; Le Page, Y.; Mc Kinnon, W. R. *Eur. J. Solid State Chem.* **1990**, *27*, 81.
(8) Tarascon, J. M.; Micelli, P. F.; Barboux, P.; Hwang, D. M.; Hull, G. W.; Giroud, M.; Greene, L. H.; Le Page, Y.; Mc Kinnon, W. R.; Tselepis, E.; Neumann, D. A.; Rhyne, J. J. *Phys. Rev. B* **1989**, *39*, 11587.
(9) Asai, K.; Yoneda, A.; Yokokura, O.; Tranquada, J. M.; Shirane, G.; Kohn, K. *J. Phys. Soc. Jpn.* **1998**, *67*, 290.

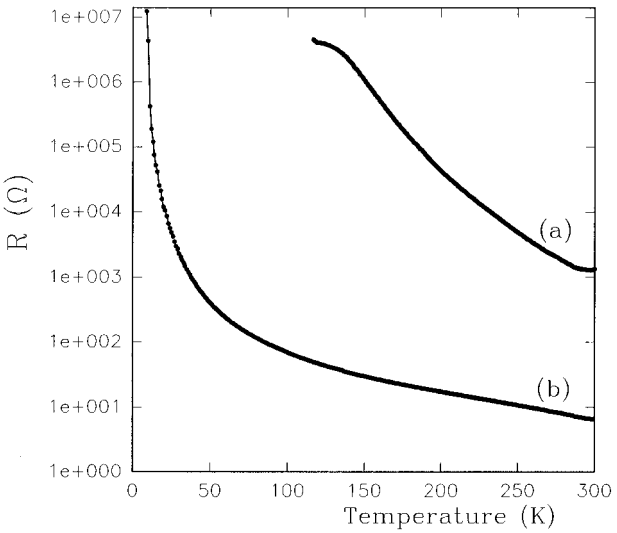

Figure 7. R = *f*(*T*) curves for as-synthesized (a) and oxygen pressure annealed (b) tubular-2 cobaltite.

as-synthesized and annealed compound (from 3.4 to 5.2 μ_B) may be the result of an oxidation of cobalt. The magnetic transition observed at 450 K suggests that a spin-state transition occurs for the trivalent cobalt. Such a Co spin-state has been extensively described in the case of $LaCoO_3$ perovskite, where the spin-state evolves from high-spin to intermediate spin at $T \approx 500$ K,[9−11] i.e., close to that of the present oxygen annealed tubular phase. The resistivity curves $\rho(T)$ of the as-synthesized and annealed samples have also been registered (Figure 7). A dramatic decrease of the room-temperature resistivity is induced by the oxygen pressure annealing from 100 Ω cm to less than 1 Ω cm, indicating an increased delocalization of the carriers induced by the oxygen uptake. However, no anomaly is detected at the magnetic transition temperature region (50−80 K). Finally, high-temperature resistivity measurements will have to be performed in order to check a possible interplay between magnetic and transport properties in the 450 K region corresponding to the magnetic transition observed for the annealed tubular cobaltite.

Concluding Remarks

This work shows that cobalt, like copper and manganese, is a potential element for the generation of tubular phases. Cobalt, like manganese, differs from copper in that the $n = 2$ member of the generic tubular series $[Bi_2Sr_2MO_6]_n[Sr_8M_6O_{16\pm\delta}]$ can be synthesized. This different behavior may be due, from a simple charge balance calculation, to the necessity for the M cation to exhibit a high oxidation state, between +2.5 and +3, which is not trivial for copper under normal synthesis conditions. Despite the existence of the two compounds $Bi_{3.6}Sr_{12.4}Mn_8O_{28.9}$ and $Bi_{3.7}Sr_{11.4}Co_8O_{26.8}$, the solid solution $Bi_{4-y}Sr_{12-z}Mn_{8-x}Co_xO_{28\pm\delta}$ does not exist in the whole substitution range; it is limited to $x \approx 2.5$. The reason of this peculiar behavior is not elucidated. It may be due to fine structural changes, associated to the changing in the space groups, in agreement with previous observations performed in the systems $LaMn_{1-x}Co_xO_3$[13] and $Bi_2Sr_2MO_{6+\delta}$ (M = Mn,Co).[7,8] A detailed structural study from neutron data and a complete magnetic study on single crystal are necessary to clarify the features of this new cobaltite phase, in particular at the level of pillars. This work is in progress and will allow a fine comparison with the corresponding manganese-based tubular phase.

Acknowledgment. The authors are grateful to Dr N. Nguyen for susceptibility measurements at high temperature.

CM980467X

(10) Stolen, S.; Gronvold, F.; Brinks, H.; Atake, T.; Mori, H. *Phys. Rev.* **1997**, *B55*, 14103.
(11) Yamaguchi, S.; Okimoto, Y.; Tokura, Y. *Phys. Rev.* **1997**, *B55*, R8666.
(12) Blasse. G. *J. Applied Phys.* **1965**, *36*, 879.
(13) Park, J. H.; Cheong, S. W.; Chen, C. T. *Phys. Rev.* **1997**, *B55*, 11072.